Int. J. Ind. Chem. 2026; 17(1): 28-40

International Journal of Industrial Chemistry (IJIC)

https://doi.org/10.57647/ijic.2026.1701.04

Research Article

A Combined Theoretical and Experimental Approach to Developing a Nickel-Selective Carbon Paste Electrode Using 2-benzamido-4-methylthiazol-5-yl Acetate as a Novel Ionophore

Nadia Tafazoli[1,2], Ashraf sadat Shahvelayati[1,2,*], Leila Hajiaghababaei[1,2,*], Jamshid Najafpour[1,2], Roya Ahmadi[1,2]

[1]*Department of Chemistry, YI.C., Islamic Azad University, Tehran, Iran*
[2]*Research Center for New Technologies in Chemistry and Related Sciences, YI.C., Islamic Azad University, Tehran, Iran*

[*]**Corresponding authors:** as.shahvelayati@iau.ac.ir, le.hajiaghababaei@iau.ac.ir

Article History:

Received:
09 January 2026

Revised:
25 February 2026

Accepted:
04 March 2026

Published in Issue:
31 March 2026

Abstract

2-benzamido-4-methylthiazol-5-yl acetate (BTA) were synthesized via an innovative synthetic route and were used for the first time, as highly selective ionophores for the development of novel potentiometric Ni^{2+} selective carbon paste electrode (CPE). First, the molecular mechanic-based MMFF94 technique was used to determine the most stable ligand BTA's conformer and its isosteric complexes with some cations. The reaction's Gibbs free energy results indicated the acceptable thermodynamic complexation reactivity of the ligand and Ni^{2+}. These results were obtained by calculating the B3LYP/6-31G(d,p), 6-31G(d,p) basis set for heavy metals substituted by LanL2DZ. The best sensor response in the case of Ni^{2+} selective CPE was obtained by 7% ionophore, 72% graphite powder, and 21% paraffin oil. The Ni^{2+} selective CPE showed a Nernstian slope of 28.4 mV/decade within the concentration range of 1.0×10^{-8} - 1.0×10^{-1} mol L^{-1}. The electrode has short response time of 4 s and can be applied as indicator electrodes in the potentiometric titration of Ni^{2+} with ethylenediaminetetraacetic acid (EDTA).

Keywords: 2-benzamido-4-methylthiazol-5-yl; Carbon paste electrode; Density functional theory (DFT); Molecular mechanics; Nickel measurement; Potentiometry

Cite this article: Tafazoli N, Shahvelayati A S, Hajiaghababaei L, Najafpour J, Ahmadi R. A Combined Theoretical and Experimental Approach to Developing a Nickel-Selective Carbon Paste Electrode Using 2-benzamido-4-methylthiazol-5-yl acetate as a Novel Ionophore. Int. J. Ind. Chem. 2026; 17(1): 28-40. https://doi.org/10.57647/ijic.2026.1701.04

1. Introduction

Nickel, a transition metal, is a lustrous, silver-white metal known for its valuable properties, including high ductility, melting point (1455 °C), and remarkable resistance to corrosion and oxidation [1]. It is ferromagnetic at room temperature and serves as a fundamental component in a vast array of industrial applications, most notably in the production of stainless steel, which accounts for approximately 65-68% of its global consumption [1,2]. Beyond metallurgy, its applications extend to rechargeable batteries, electroplating, catalysts, and aerospace superalloys, underscoring its critical role in modern industry and the burgeoning green energy

transition [3]. However, the increasing extraction and utilization of nickel have led to significant environmental and health concerns. The environmental impact of nickel begins at the source, with mining and processing operations causing deforestation, siltation of rivers, and dust pollution that harms local ecosystems, fisheries, and agricultural land [4].

From a toxicological perspective, nickel and its compounds, particularly in dust and fume forms, are hazardous. Inhalation can cause respiratory problems, chronic bronchitis, and lung fibrosis, while certain nickel compounds are classified as human carcinogens. Dermal contact can also lead to allergic reactions known as "nickel itch". The contamination of water bodies with nickel ions from industrial effluent is particularly concerning, as it can be harmful to aquatic life and enter the food chain [1,5].

Analytical methods such as atomic absorption spectroscopy (AAS) [6], X -ray fluorescence (XRF) [7], inductively coupled plasma-optical emission spectroscopy (ICP-OES) [8,9] and UV-Vis. spectroscopy [10,11] are performed to determine the trace level of metals like nickel. Nevertheless, these procedures have some disadvantages based on the cost and time of routine analysis and the tedious sample preparation process [5, 12-13]. Hence, the search for new simple and rapid methods for heavy metal measurement is a challenging goal.

In this regard, potentiometric ion selective electrode (ISE) can be a leading alternative for the stated complicated approaches. Several types of potentiometric ion-selective electrodes exit, such as ion-selective electrodes with internal liquid electrolyte, coated wire ion selective electrodes, carbon paste ion selective electrodes, solid-state ion selective electrodes, and field-effect transistors (FET) [14-17]. On this matter, potentiometric carbon paste electrodes (CPE) are extensively used as simple instruments for detecting different analytes regarding their facile construction, higher signal-to-noise ratio, easy renewability of the surface, stability of response, low-cost methods, lower ohmic resistance, and not requiring the internal solution [18-20].

More prominently, carbon paste electrodes can be simply modified with different kinds of inorganic or organic modifiers by only mixing the modifier with binder and carbon in the paste preparing stage. The electrode's surface state can be improved by modification, which significantly increases the target signals [21]. The potentiometric CPEs' ion-sensing features are primarily based on the utilized sensing materials' nature [22].

Over the last decades, several inorganic and organic compounds have been used in the literature as ionophores for preparing selective nickel electrodes. Dimethylglyoxime and Ethylenediamine [23], N, N′-bis(4-dimethylamino-benzylidene)-benzene-1,2-diamineand [24], 2-((5-(2-hydroxy-3-methoxybenzylideneamino)-2H-1,2,4-triazol-3-ylimino) methyl)-6-methoxyphenol [25], 1,10-Phenanthroline [26], Asparagine and L-Methionine [27], Macrocyclic / heterocyclic [28] have all been used as ionophores for designing nickel selective electrodes. However, many of these electrodes have some defects like short life span, long response time, high limit of detection, serious interference from other cations, and a narrow working pH range. Therefore, more studies are required in this field to reach more effective electrodes with better features and enhance the position of ISE in routine analysis.

In this research, we synthesized 2-benzamido-4-methylthiazol-5-yl acetate (BTA) in two steps for the first time and used it as new ionophore to fabricate modified carbon paste electrodes for measurement of the Ni^{2+} ions potentiometrically. To the best of our knowledge, this is the first ion selective CPE, prepared with this ionophore as the recognition element of the electrode.

Considering to chemical computational methods can greatly help evaluate thermodynamic parameters and reaction mechanism exploration [29], before fabrication of the electrode, the molecular mechanics force field (MMFF94) technique was used to determine the most stable conformer of the 2-benzamido-4-methylthiazol-5-yl acetate (BTA) and its isosteric complexes with some of the cations.

The theoretical thermodynamics of the reactions between some cations with the most stable conformer BTA was investigated in gas phases through the B3LYP/6-31G (d, p) computational level [30]. Next, for all cations, except Hg^{2+}, Ag^{+}, and Pb^{2+}, the DFT/B3LYP/6-31G(d,p) computational levels were used for applying the B3LYP/LANL2DZ level [31].

2. Experimental

2.1. Apparatus

A Bruker Tensor 27 tool was used to record Fourier transform infrared spectra utilizing KBr disks. Also, an ultra-shield Bruker 400 instrument was used to record ^{1}H and ^{13}C nuclear magnetic resonance (NMR) spectra via DMSO as the deuterated solvent. LG microwave MP-9484WCR model for synthesis of Ionophore was used. A Bransetead Electro Thermal B1 tool was used to determine the melting point.

Also, the constructed ion-selective CPE, as the working electrode, was placed in a glass cell along with a double junction Ag/AgCl as the reference electrode for potentiometric measurement. The two electrodes were linked to a digital milli-voltmeter (HIOKI 3256.50) with ± 0.1 mV precision. The pH controlling was performed using a Metrohm pH-meter with a combined glass electrod

10.57647/ijic.2026.1701.04

2.2. Reagents and materials

Benzoyl chloride, Potassium thiocyanate, acetonitrile, Anhydride acetic, alanine and high-purity paraffin oil were purchased from Sigma-Aldrich. The used nitrate salts of the cations (from Merck and Sigma-Aldrich) had the highest available purity. All experiments were performed using double distilled deionized water. Detections were performed by applying iodine vapor in the thin layer chromatography (TLC).

2.3. Synthesis of Ionophore

The ionophore was synthesized in two steps:

A: Synthesis of benzoylcarbamothioyl alanine

Benzoyl chloride and potassium thiocyanate were reacted in acetonitrile at room temperature for 20 minutes. After filtration to remove the precipitated KCl, alanine (1 mmol) was added and reacted with the in situ generated benzoyl isothiocyanate (1 mmol) in 10 mL of acetonitrile under reflux at 80 °C for 24 hours. The reaction completion was monitored by thin-layer chromatography (TLC). Then, after evaporation of the solvent, the benzoylcarbamothioyl alanine product was used in the next step without further purification (Scheme 1).

B: Synthesis of 2-benzamido-4-methylthiazol-5-yl acetate (BTA)

In a typical procedure, benzoylcarbamothioyl alanine (1 mmol) was dissolved in acetic anhydride (2 mL) and irradiated with microwaves at 100 °C for 15 minutes. Upon completion of the reaction, the mixture was quenched with water. The resulting yellowish crude residue was purified by dry-flash chromatography using a 1:3 mixture of n-hexane/ethyl acetate as the eluent, yielding the corresponding product, 2-benzamido-4-methylthiazol-5-yl acetate. This compound, after purification and structural confirmation by melting point determination, FT-IR, ^{13}C-NMR, and ^{1}H-NMR spectroscopy, was used in the preparation of composite carbon paste electrodes (CPEs) (see Scheme 2).

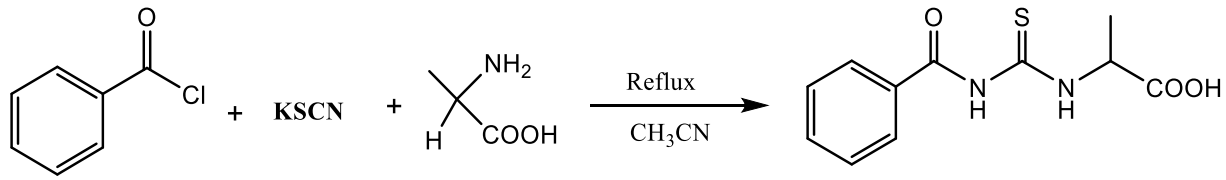

Scheme 1. Synthesis of benzoylcarbamothioyl alanine

White powder, m.p. 180-182 °C; yield: 0.24 g (97%). IR (KBr): 3300, 1683, 1620, 1200, 1120 cm^{-1}. ^{1}H NMR: δ =1.49 (3 H, d, ^{3}J = 7.5, Me), 4.85 (1 H, quintet, ^{3}J = 7.5, CH), 7.48 (2 H, t, ^{3}J = 7.2, 2 CH), 7.60 (1 H, t, ^{3}J = 7.2, CH), 7.92 (2 H, d, ^{3}J = 7.2, 2 CH), 11.30 (1 H, d, ^{3}J = 7.5, NH), 11.36 (1 H, s, NH) ppm. ^{13}C NMR: δ = 17.2 (Me), 53.2 (CH), 128.3 (2 CH), 128.5 (2 CH), 132.1 (C), 132.9 (C), 168.0 (C=O), 172.9 (C=O), 179.8 (C=S) ppm

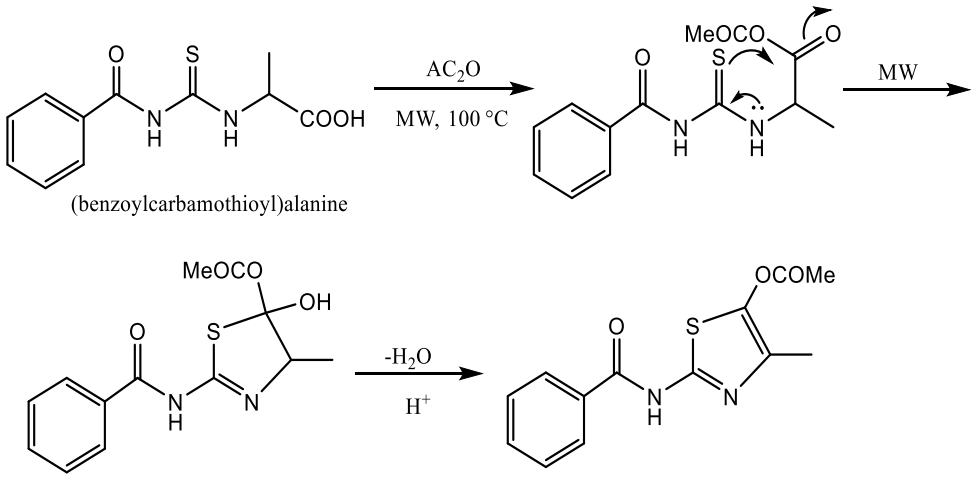

Scheme 2. Synthesis of 2-benzamido-4-methylthiazol-5-yl acetate (BTA)

White powder, m.p. 186-187 °C; yield: 0.23 g (84%). IR (KBr): 3373, 3001, 1731, 1675, 1518, 1172, 1141 cm^{-1}. ^{1}H NMR (300 MHz, DMSO): δ =1.93 (3 H, s, Me), 2.35 (3 H, s, Me), 7.50 (2 H, t, ^{3}J = 7.0, 2 CH), 7.59 (1 H, t, ^{3}J = 7.0, CH), 7.93 (2 H, t, ^{3}J = 7.0, 2 CH), 11.28 (1 H, br s, NH) ppm. ^{13}C NMR (75 MHz, DMSO): δ = 13.2 (Me), 20.8 (Me), 127.6 (2 CH), 128.2 (2 CH), 129.3 (CH), 132.5 (C), 133.2 (C), 137.3 (C), 152.8 (C=N), 165.5 (C=O), 167.8 (C=O) ppm. Anal. Calcd for $C_{13}H_{12}N_2O_3S$ (276.06): C, 56.51; H, 4.38; N, 10.14; Found: C, 59.40; H, 5.08; N, 9.89

10.57647/ijic.2026.1701.04

2.4. Computational Evaluation

The ligand (BTA) was built and searched for the initial conformational by adopting the Spartan'10 software [32] with MMFF94. Next, its isosteric complexes with cations were defined using the MMFF94 technique. From many guess structures, the conformer with the lowest Gibb's free energy was obtained by applying the Maxwell-Boltzmann equation [33]. The Gauss view 5.0 software [34] was used to clarify output files from the Spartan program. Using Density Functional Theory (DFT), binding energies of BTA with the different cations were computationally evaluated, and the mechanism of the sensor toward nickel was demonstrated. The calculations were made using DFT performed using the exchange-correlation potential made. To this end, we used Becke's three-parameter functional for exchange (B3) [35, 36] along with the Lee-Yang-Parr (LYP) correlation parametrization as implemented B3LYP technique [37] with 6-31G(d,p) combined with LANL2DZ basis set using Gaussian 09 software [38] in the gaseous.

For all cations except Hg^{2+}, Ag^{+}, and Pb^{2+} calculations were performed by applying the Los Alamos National Laboratory of Double Zeta (LanL2DZ) basis set using the 6-31G(d,p) basis set. The thermodynamic quantities of all components were evaluated by calculating the second derivatives of the energy with respect to the structural variables (harmonic frequencies) at the same theoretical level for confirming the kind of stationary point (local minima) [39]. No imaginary frequency was observed for the considered structures (Table 1).

Accordingly, the lowest frequency is obtained for the complex of the mercury ion with ligand (16.058 cm^{-1}). No symmetry constraints were imposed during geometry optimization. Full geometry optimizations were carried out in both gas and aqueous phases. Solvent effects were included using the IEFPCM model [40] with water as solvent. The binding energy was calculated according to Eq. (1).

$$\Delta E = \Delta E_{complex} - (\Delta E_{Ligand} + \Delta E_{cation}) \quad (1)$$

2.5. Electrode preparation

For fabricating the modified CPE, the pastes were prepared by hand-mixing different amounts of the synthesized ionophore powder and various amounts of graphite, and paraffin oil for 20 min. When each mixture was homogenized, a portion of the prepared paste was carefully packed into the tube tip to prevent possible air gaps. It regularly improves the electrode resistance. Electrical contact was established by inserting a copper wire into the CPE opposite end. Before usage, a piece of soft paper was used to smooth the carbon paste's external surface. The old surface was scraped out, and the new carbon paste was replaced to make a new surface. The electrode was ultimately conditioned for 24 h by soaking in a 1.0×10^{-3} mol L^{-1} of analyte solution.

2.6. Emf Measurements

The potential difference is proportional to the ion activity logarithm based on the Nernst equation [41]. Also, potentiometric measurements were performed by determining the potential difference between CPE and reference electrode using a multi-meter with a volt-meter with ±0.1 mV precision at room temperature. The electrochemical cells used are represented as follows: Developed carbon paste electrode | sample solution || Ag−AgCl, KC1 (satd.)

3. Results and Discussion

In the present work, 2-benzamido-4-methylthiazol-5-yl acetate was synthesized via an innovative synthetic route and was used, for the first time, as highly selective ionophore for the development of novel potentiometric Ni^{2+}-selective carbon paste electrode. To this end, the theoretical thermodynamics of the reactions between some ions with BTA was investigated.

3.1. Theoretical study

The computations were performed for each reactant (Ligands and Cations) and products (Complexes) in the reaction: Ligand + Cations → Complex.

Conformational analysis revealed that the free BTA ligand adopts five distinct conformers. Upon complexation, six low-energy conformers (A–F) are accessible for Ni^{2+}, Fe^{2+}, and Zn^{2+}. In contrast, for Hg^{2+}, Pb^{2+}, and Ag^{+}, the D and E conformers are not minima on the potential energy surface; instead, two new conformers (G and H) emerge as the most stable alternatives, effectively replacing D and E. Thus, while the initial search space includes A–F for all metals, the final conformational ensemble differs: A–F for Ni/Fe/Zn, and A, B, C, F, G, H for Hg/Pb/Ag.

In the first step, the reaction in the gas phase was investigated. Next, the reaction was studied in the solution (liquid) phase. In the liquid phase, ligand and complexes are studied in water solvent. The thermochemistry outputs in the best stable structure complex (with the lowest total energy) in the gas (the first line in each row) and solvent phase (the second line in each row) are represented in Table 1.

In this table, ΔS_{th}, ΔH_{th}, and ΔG_{th} are the changes of thermal corrections to the entropy, enthalpy, and Gibbs free energy, respectively, and $\Delta G°$ shows Gibbs free energy at standard state (298 K and 1 atm).

10.57647/ijic.2026.1701.04

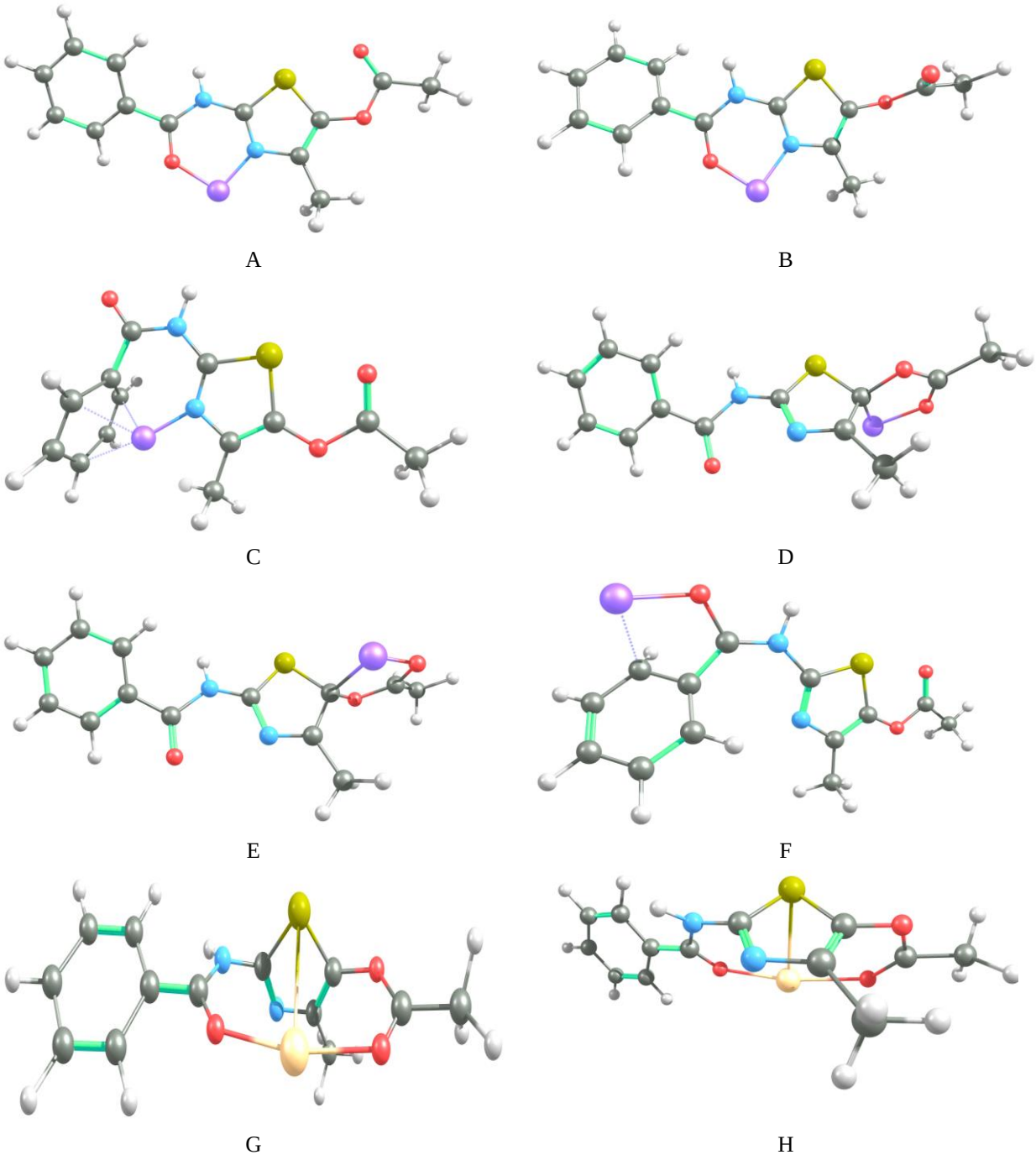

Figure 1. Optimized geometries of the six possible conformers (A–F) of the BTA–Ni^{2+} complex obtained at the B3LYP/6-31G(d,p)/LANL2DZ level of theory in the gas phase. These conformers serve as the reference set for all six metal ions. For Ni^{2+}, Fe^{2+}, and Zn^{2+}, they constitute the full conformational ensemble. For Hg^{2+}, Pb^{2+}, and Ag^{+}, conformers D and E are not stable and are replaced by two new structures (G and H)
Color code: Ni (purple), C (gray), H (white), N (blue), O (red), and S (yellow)

The Gibbs free energy thermal was corrected by adding the entropy term to the thermal correction of enthalpy ($\Delta G_{th} = \Delta H_{th}-T\Delta S_{th}$) [42].

Eventually, Gibbs free energy is obtained as the sum of the total electronic energy variation in the reaction as well as thermal correction of the Gibbs free energy ($\Delta G° = \Delta\varepsilon_o + \Delta G_{th}$) [43]. The changes in the thermal correction to the entropy of complexes formation from all cations with the ligand are negative, except for Hg^{2+} and Ag^{+} in solvent phase. Therefore, the mentioned complexation reaction's entropy caused by aggregation in the complex is not proper in liquid phase. However, the reaction's enthalpy at the standard state ($\Delta H° = \Delta\varepsilon_o + \Delta H_{th}$) is proper to react between ligand and cations and create the complex. The explanation is that the enthalpy of the formation of reaction complexes from all ion metals with the ligand is negative at the standard state.

Overall, the reaction Gibbs free energy order of the thermodynamic reactivity of cations complexation with stable ligand in the gas phase (with the lowest total energy) is as follows: $Ni^{2+} > Fe^{2+} > Zn^{2+} > Hg^{2+} > Pb^{2+} > Ag^{2+}$ respectively. (Table 1).

10.57647/ijic.2026.1701.04

Table 1. Calculated thermochemical parameters for the complexation reaction *Ligand* + *Cation* → *Complex* evaluated for the first local minimum complex (lowest total energy) using DFT calculations. For each complex, three sets of values are reported: **(i)** gas-phase calculations in which the ligand, cation, and complex are all considered in the gas phase (first line), **(ii)** solution-phase calculations in which the ligand, cation, and complex are all considered in the aqueous phase (second line), and **(iii)** mixed-phase calculations in which the ligand is considered in the gas phase while the cation and complex are considered in the aqueous phase (third line). Calculated values include $\Delta\varepsilon^0$, $\Delta H°$, ΔS_{th}, $\Delta G°$, the lowest vibrational frequency of the optimized complex, and the corresponding conformer label.

Complexes	$\Delta\varepsilon_0$ (kcal/mol)	ΔH° (kcal/mol)	ΔS_{th} (cal/mol.K)	ΔG° (kcal/mol)	lowest freq. of complex (Cm^{-1})
	-344.214	-343.840	-38.953	-332.227	30.564
Ni^{2+}	-90.576	-88.741	-88.741	-76.708	35.157
	-107.924	-106.312	-40.851	-94.133	35.157
	-331.262	-331.183	-42.831	-318.414	31.778
Fe^{2+}	-78.599	-76.895	-44.188	-63.720	29.469
	-95.946	-94.466	-44.681	-81.145	29.469
	-281.172	-280.658	-35.718	-270.009	35.007
Zn^{2+}	-41.251	-40.140	-34.657	-29.808	31.387
	-58.599	-57.712	-35.150	-47.232	31.387
	-202.367	-202.840	-32.857	-193.044	30.952
Hg^{2+}	18.350	18.975	-28.434	27.452	16.058
	1.003	0.401	158.181	10.028	16.058
	-180.706	-180.317	-35.195	-169.824	31.150
Pb^{2+}	-42.472	-41.309	-34.594	-30.995	30.629
	-59.820	-58.880	-35.087	-48.420	30.629
	-56.681	-56.032	-30.613	-46.906	28.506
Ag^{+}	6.051	6.819	-28.922	15.442	23.160
	-11.297	-10.752	-29.415	-1.983	23.160

Table 2. Boltzmann-averaged thermochemical parameters for the complexation reaction *Ligand* + *Cation* → *Complex* calculated over all accessible conformers of each BTA–metal complex using the Maxwell–Boltzmann distribution. For each complex, three sets of values are reported: **(i)** gas-phase calculations in which the ligand, cation, and complex are all considered in the gas phase (first set), **(ii)** aqueous-phase calculations in which the ligand, cation, and complex are all considered in the aqueous phase (second set), and **(iii)** mixed-phase calculations in which the ligand is considered in the gas phase while the cation and complex are considered in the aqueous phase (third set). Reported values include $\Delta\varepsilon^0$, $\Delta H°$, ΔS_{th}, and $\Delta G°$

Complexes	$\Delta\varepsilon_0$ (kcal/mol)	ΔH° (kcal/mol)	ΔS_{th} (cal/mol.K)	ΔG° (kcal/mol)
	-344.210	-343.835	-38.954	-332.221
Ni^{2+}	-90.560	-88.716	-40.755	-76.565
	-107.908	-106.287	-41.248	-93.989
	-331.262	-331.183	-42.830	-318.414
Fe^{2+}	-78.599	-76.895	-44.191	-63.719
	-95.946	-94.466	-44.683	-81.144
	-281.172	-280.658	-35.717	-270.009
Zn^{2+}	-41.272	-40.134	-34.826	-29.751
	-58.619	-57.705	-35.318	-47.175
	-202.362	-202.832	-33.296	-192.905
Hg^{2+}	18.461	19.048	-15.679	23.722
	1.114	1.476	-28.719	10.039
	-180.706	-180.317	-35.193	-169.824
Pb^{2+}	-62.873	-41.303	-35.071	-30.846
	-59.835	-58.874	-35.563	-48.271
	-56.668	-56.012	-30.612	-46.885
Ag^{+}	5.998	6.759	-29.231	15.474
	-11.350	-10.813	-29.723	-1.951

Also, the reaction Gibbs free energy order of the thermodynamic reactivity of complexation of cations with stable ligand in solvent phase (with the lowest total energy) was obtained as follows: Ni^{2+} > Fe^{2+} > Pb^{2+} > Zn^{2+} > Ag^{+} > Hg^{2+} (Table 1). For the mixed-phase calculations (ligand in gas phase, cation and complex in

10.57647/ijic.2026.1701.04

aqueous phase), the same ordering is observed.

Notably, when Boltzmann-averaged over all accessible conformers (Table 2), the ordering remains identical to Table 1 in both aqueous and mixed phases, while the gas-phase ordering persists unchanged — confirming the robustness of the aqueous-phase trend.

Table 3 lists the metal–donor distances in the lowest-energy conformer, as identified by the global minimum in Table 1, for both gas and aqueous phases, with heteroatom numbering defined in Fig. 2. The coordination mode clearly depends on the metal ion and preferred conformer. For Ni^{2+} and Zn^{2+} (Conf. A in Fig. 1), the shortest distances correspond to M–O1 and M–N2, indicating bidentate coordination through O1 (carbonyl oxygen) and N2 (thiazole nitrogen).

In contrast, the most stable Fe^{2+} complex adopts Conf. C in Fig. 1, in which the metal ion primarily interacts with the thiazole nitrogen (M–N1 ≈ 1.83 Å), while the distances to oxygen and sulfur atoms remain significantly longer. This suggests a different coordination mode dominated by nitrogen donation and possible π-interaction with the aromatic system. This structural distinction is consistent with the thermodynamic data, where Fe^{2+} still exhibits highly negative ΔG° values despite the absence of strong metal–oxygen interactions. For Hg^{2+}, the global minimum in aqueous phase corresponds to Conf. G (not A), as confirmed by the energy ordering in Table 1 and the structural data in Table 3. Notably, this conformational switch results in significantly longer M–donor distances (e.g., M–O1 = 3.380 Å), leading to weaker coordination and ultimately rendering the complex thermodynamically unstable in water (ΔG° = +10.028 kcal/mol), making it the least stable complex in aqueous medium.

3.2. Sensing Element Composition

The Nernstian response of an ion-selective electrode is a function of its composition [44]. Therefore, the effect of the paste composition on the modified CPE potential responses was investigated. To this end, several electrodes were fabricated with various compositions (Table 4). Unmodified CPE was made by combining 75% of graphite powder with 25% of paraffin. Based on the obtained results, the electrode without the ionophore represented poor sensitivity to Nickel. Also, the graphite powder was combined with a favored weight of ligand, as given in Table 4.

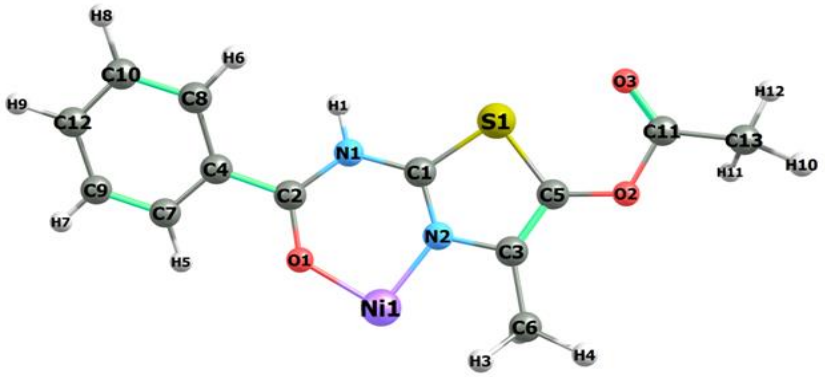

Figure 2. The most stable equilibrium geometry of 2-benzamido-4-methylthiazol-5-yl acetate(ligand) with (Ni^{2+})

Table 3. Metal–donor distances (Å) for the lowest-energy conformer of each complex, determined as the global minimum in Table 1, in gas phase (values in parentheses: aqueous phase). Heteroatom numbering follows Fig. 2

Complex	M-S	M-N1	M-N2	M-O1	M-O2	M-O3	Conf.
Ni^{2+}	4.284	3.134	1.754	1.752	5.017	6.374	A
	(4.335)	(3.104)	(1.814)	(1.770)	(5.196)	(6.573)	A
Fe^{2+}	4.409	1.834	3.346	5.093	4.237	6.52	C
	(4.488)	(1.929)	(3.358)	(5.292)	(4.262)	(6.710)	C
Zn^{2+}	4.310	2.933	1.871	1.827	5.355	6.548	A
	(4.449)	(3.139)	(1.961)	(1.934)	(5.398)	(6.741)	A
Hg^{2+}	5.008	3.680	2.512	2.356	5.749	7.193	A
	(3.683)	(5.070)	(5.924)	(3.380)	(5.481)	(3.927)	G
Pb^{2+}	4.824	3.551	2.280	2.117	5.629	6.994	A
	(4.871)	(3.596)	(2.334)	(2.174)	(5.669)	(7.109)	A
Ag^{+}	4.796	3.499	2.268	2.293	5.656	7.053	A
	(4.904)	(3.649)	(2.349)	(2.393)	(5.686)	(7.171)	A

10.57647/ijic.2026.1701.04

As can be seen, an increase in ligand level in the CPE (no.1-3) from 2 to 7 percent led to an increased slope of the calibration curve for nickel selective electrode from 5.3 mV/decade to 28.44 mV/decade. It was revealed that the quantity of the ionophore is the key factor in the suggested carbon paste electrodes with the main role in the potential response of the sensors. Improving the response of electrodes by increasing the ionophores amounts shows the affinity of the ligand to nickel ions [44]. But more increase in the ligand (no. 4) lowered the calibration curve slope for nickel selective electrode, which can be due to heterogeneity in the carbon paste. Accordingly, a composition of 7% of ligand, 72% graphite powder and 21% paraffin oil were found to have the best performance and was chosen as the optimal composition for Ni^{2+} electrode.

3.3. Calibration curve of nickel-selective CPE

To improve the linear range of the CPE, we immobilized the best composition of the carbon paste. The Nernstian slope is a very interesting factor in discovering whether ion-selective electrodes are conveniently employed in analytical applications. This value is estimated using the slope curve of the potential measured in (EMF/mV) against the log activity of the standard solution (M) (Fig. 3). The optimal value of 59.10/n (mV/decade) was obtained for the Nernstian slope [45], where (n) is the valency of nickel.The potential response of electrode showed a linear concentration range of 1×10^{-1} to 1×10^{-8} mol/L for Ni^{2+} ion in the calibration solutions with Nernstian slop of 28.4 mV/decade (Fig. 3). The LOD values were calculated by substituting the potential value, which is the projection of the cut-off point in the correct equation [46]. The electrode displays a low LOD of 8.1×10^{-9} mol/L for proposed CPE.

3.4. The response time of nickel-selective CPE

Response time is used to characterize each sensor based on the time required by the potential response to obtain values within ±1 mV of the final equilibrium potential [47]. These values are obtained by recording the potential alterations of the nickel electrodes to obtain a potential within ±1 mV of the ultimate equilibrium value, followed by the successive immersion in a series of Ni^{+2} solutions, each with 10-fold different concentrations. The sensor could quickly reach it equilibrium response in the complete concentration range. In the whole concentration range, the average response time was 4 s for CPE (Fig. 4). The quick exchange kinetics of complexation-decomplexation of Ni^{2+} ion with the ionophore at the boundary of membrane-solution can be created at this duration.

3.5. The pH dependence of Nickel selective CPE

The effect of pH on the electrode response was examined by determining the potential at the nickel solution (0.1 mM) specific concentration from the pH of 2.0 to 11.0. To this end, pH was adjusted by concentrated NaOH or HCl solutions. According to the results, the potential is constant at pH = 5.0-7.5 (Fig. 5), representing the performance of the CPE in this pH range. The changes above and below this range may be caused by the creation of $Ni(OH)_2$ and the response to proton ions respectively.

Table 4. The optimization of the membrane ingredients

NO.	% Ionophore	% Graphite	% Paraffin oil	Slope, mV/decade	Working Range, M
1	2	73	25	5.3	1×10^{-1}- 1×10^{-8}
2	5	70	25	12.2	1×10^{-1}- 1×10^{-8}
3	7	72	21	28.4	1×10^{-1}- 1×10^{-8}
4	10	65	25	14.6	1×10^{-1}- 1×10^{-8}

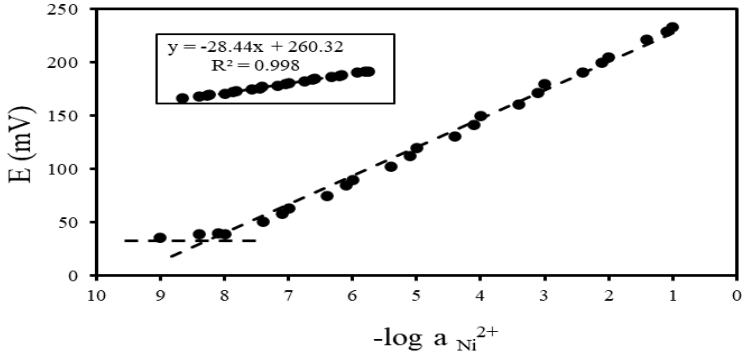

Figure 3. Calibration curve and LOD of nickel CPE

10.57647/ijic.2026.1701.04

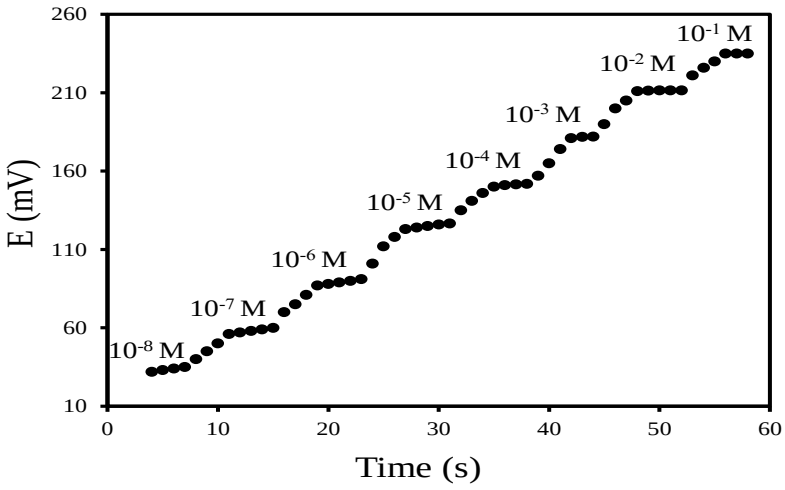

Figure 4. Response time of proposed CPE in various concentration of Ni^{2+}

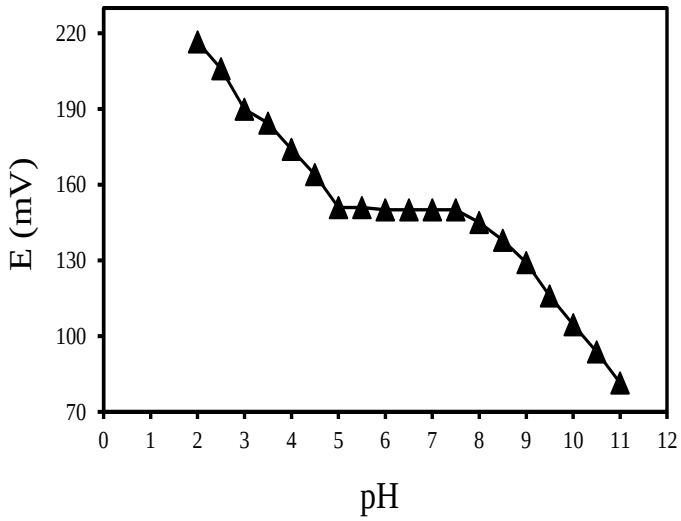

Figure 5. pH effect on electrodes responses

3.6. Selectivity and interference

Response to the target ion is among the most remarkable features of any ion selective electrode. This feature, which is determined over other species and ions existing in the solution, is known as the potentiometric-selectivity coefficient. We used the matched potential method (MPM) for assessing the developed sensor's selectivity coefficients [48, 49] (Table 5). A K_{MPM} value of 1.0 indicates the sensor with similar responses to both the interfering and primary ions, while smaller values denote higher selectivity. All the results are less than 10^{-3}, representing the developed sensors' higher selectivity for the target ion.

3.7. Life Time of the Electrode

The lifetime of the proposed CPE was assessed by recalibration in standard solutions periodically and calculation of the optimized electrode's slope within some weeks in the linear concentration range of each of the electrode. During this period, the CPE were used weekly. The suggested electrode was washed gently with distilled water, dried, and kept at room temperature.The obtained results revealed that the Ni^{2+} selective CPE could be used for 12 weeks with no considerable changes in its slope. By the end of this time, there was a slight gradual reduction in the slopes, indicating that the lifetime of the presented nickel selective CPEs were 3 months, at least.

3.8. Analytical Applications

The analytical utility of nickel-selective CPE was established using it as an indicator electrode for potentiometric titration of 25 mL 1.0×10^{-4} mol/L Ni^{2+} solution with 1.0×10^{-2} mol/L ethylenediaminetetraacetic acid (EDTA). According to Fig. 6, increasing the quantity of EDTA reduces the potential values because of forming complexation between nickel ions with EDTA and decreasing the free nickel ions concentration in solution. This nickel CPE could act as indicator electrodes regarding the sharp endpoint in the titration curve.

10.57647/ijic.2026.1701.04

Table 5. The selectivity coefficients of various interfering cations for Ni^{2+} selective CPE

Ion	K_{MPM}	Ion	K_{MPM}
Co^{2+}	1.3×10^{-5}	Zn^{2+}	1.4×10^{-5}
Cu^{2+}	3.0×10^{-5}	Ag^{+}	1.2×10^{-5}
Fe^{2+}	1.6×10^{-5}	Pb^{2+}	6.3×10^{-5}
Ca^{2+}	8.3×10^{-5}	Mg^{2+}	1.2×10^{-5}
Cd^{2+}	9.2×10^{-4}	Hg^{2+}	7.1×10^{-4}
Cr^{3+}	1.4×10^{-5}	Mn^{2+}	1.3×10^{-5}

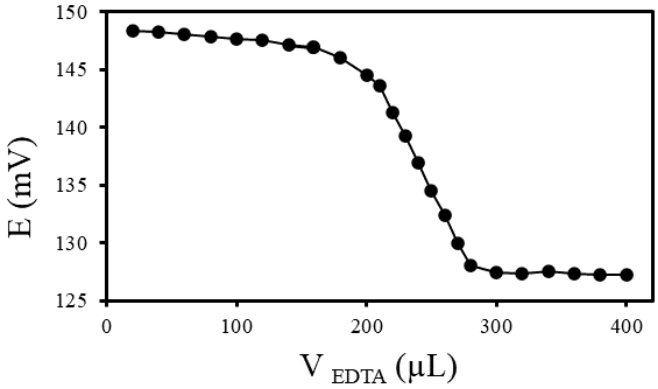

Figure 6. Potential titration curve of 25 mL 1.0×10^{-4} mol/L Ni^{2+} solution with 1.0×10^{-2} mol/L of EDTA by using CPE

Table 7. Comparison between some characteristics of the proposed CPE and previously reported Nickel electrodes

Ionophore	Slope (mV/ decade)	W.R. (M)	D.L. (M)	Working pH range	R.T. (s)	S.I.	Ref.
(2E,3E)-2H-1,4-benzothiazine-2,3(4H)-dione	28.2	1.0×10^{-6} to 1.0	1.6×10^{-6}	2.0–6.5	<10	Cd^{2+}, Zn^{2+}, Cu^{2+}, Co^{2+}, Pb^{2+}	[50]
N,N′-bis(salicylidene)-2-aminobenzylamine	29	1.0×10^{-6} to 1.0×10^{-1}	6.3×10^{-7}	2.0–9.8	≥10	Hg^{2+}, Cu^{2+}, Pb^{2+}	[51]
N-(2-Hydroxybenzylidene) -N′-(2-picolyl)eth	29	8.51×10^{-6} to 1.0×10^{-1}	8.51×10^{-6}	3.5–7.5	7–12	Co^{2+}, Cu^{2+}, Zn^{2+}, Fe^{3+}	[52]
1,2,4-Triazole bis Schiff base'	29.3	1.0×10^{-7} to 1.0×10^{-1}	3.0×10^{-8}	3.0–8.0	11	Cu^{2+}, Co^{2+}, Zn^{2+}, Cd^{2+}	[53]
2-benzamido-4-methylthiazol-5-yl acetate	28.4	1.0×10^{-8} to 1.0×10^{-1}	8.1×10^{-9}	5.0-7.5	3	———	This Work

R.T.: Response Time, D.L.: Detect Limit, W.R.: Working Range, S.I.: Significant Interference

3.9. Comparison with Previous Studies

A comparison was made between the efficiency of several of ion selective electrodes using various ionophores and the analytical performance of nickel selective CPE developed in this study (Table 7) [50-53]. Proposed CPE offers better features than mentioned electrodes in the response time, working range, and LOD. Also, this CPE has shown superior selectivity toward Ni^{2+} over most interfering cations studied. The good selectivity of developed CPE may be due to the 2-benzamido-4-methylthiazol-5-yl acetate as an ionophore. 2-benzamido-4-methylthiazol-5-yl acetate molecule serves as a selective ligand for Ni^{2+} ions. The only disadvantage of proposed CPE is narrow working pH range in comparison with other electrodes.

4. Conclusion

For the first time, 2-benzamido-4-methylthiazol-5-yl acetate was synthesized and used as a neutral carrier to design carbon paste potentiometric electrode for Ni^{2+} determination. The interaction between BTA and Ni^{2+} ions was studied theoretical and experimental. The theoretical

10.57647/ijic.2026.1701.04

results showed that the ligand is highly inclined to react with Ni^{2+}. The coordination mode clearly depends on the metal ion and preferred conformer. For Ni^{2+}, indicating bidentate coordination through carbonyl oxygen and thiazole nitrogen. In experimental study, Graphite, Paraffin oil, and ionophore were applied in Ni^{2+} selective carbon paste electrode with an optimal ratio of 72:21:7, which led to a Nernstian slope of 28.4 mV/decade. Limit of detection method was 8.1×10^{-9} M. Also, response time and lifetime of CPE was approximately 4 s and 12 weeks, respectively. Eventually, the designed electrodes were successfully applied in determination of nickel ions as indicator electrode in potentiometric titration of $Ni^{2+}$with EDTA.

Acknowledgments

The author thanks the Research Council of the Islamic Azad University of Yadegar-e-Imam Khomeini (RAH) Shahre Rey branch for supporting this work.

Authors Contribution

Conceptualization, A.S. and L.H.; Methodology, A.S. and L.H. and J.N.; Software and modeling, J.N.; Validation and Formal analysis, N.T.; Investigation, Resources, Data curation, N.T.; Writing – original draft, N.T.; Writing – review and editing, A.S. and L.H. and J.N.; Supervision and Project administration, A.S. and L.H.; All authors have read and approved the final version of the manuscript

Availability of data and materials

The data that support the findings of this study are available from the corresponding author, upon reasonable request.

Conflict of interests

The author states that there is no conflict of interest.

References

[1] Begum W, Rai S, Banerjee S, Bhattacharjee S, Mondal MH, Bhattarai A, et al. *A comprehensive review on the sources, essentiality and toxicological profile of nickel.* RSC Adv. 2022;12(48):31384-31406. http://doi.org/10.1039/D2RA05104D

[2] Yonezawa T. Nickel-based alloys. In: Konings RJM, Stoller RE, editors. *Comprehensive nuclear materials*. 2nd ed. Amsterdam: Elsevier; 2020. p. 1-38. http://doi.org/10.1016/B978-0-12-803581-8.00676-7

[3] Li Y, Liu X, Chen M. *Nickel-based materials: toward practical application of the aqueous hybrid supercapacitors*. Sustainable Mater Technol. 2022;33: e00467. http://doi.org/ 10.1016/j.susmat. 2022.e00467

[4] Wang J, Li Z, Zhang Y, et al. *Enhancing corrosion resistance of nickel-based alloys: a review of alloying, surface treatments, and environmental effects*. J Alloys Compd. 2025;1725757. http://doi.org/ 10.1016/j.jallcom.2025.1725757

[5] Zhang X, Wang H, Liu Q. *A comprehensive review of microstructural heterogeneities in the laser powder bed fusion of nickel-base superalloys with high γ′ content.* Acta Mater. 2024; 275:120047. http://doi.org/ 10.1016/j.actamat.2024.120047

[6] Tokalıoğlu Ş, Papak A, Şahan A. *Designing a simple semi-utomated system for preconcentration and determination of nickel(II) using dispersive liquid–liquid microextraction with flame atomic absorption spectrometry*. Arab J Chem. 2022;15(10):104007. http://doi.org/ 10.1016/j.arabjc.2022.104007

[7] Verma P, Kalra N, Verma S. *Advancement in sensory identification of heavy metal contamination in water: a review on progression from spectroscopic analytical techniques to handheld sensors.* Microchem J. 2024; 205:111293. http://doi.org/ 10.1016/j.microc.2024.111293

[8] Gazulla MF, Ventura MJ, Orduña M, Rodrigo M, Torres A. *Determination of trace metals by ICP-OES in petroleum cokes using a novel microwave assisted digestion method*. Talanta Open. 2022; 6:100134. http://doi.org/ 10.1016/j.talo.2022.100134

[9] Robert-Peillard F, El Mouchtari EM, Bonne D, Humbel S, Boudenne JL, Coulomb B. *Determination of dissolved nickel in natural waters using a rapid microplate fluorescence assay method*. Spectrochim Acta Part A. 2022; 275:121170. http://doi.org/ 10.1016/j.saa.2022.121170

[10] Soylak M, Ahmed HEH, Goktas O. *Dispersive micro-solid phase extraction (D-μSPE) of nickel on activated nanodiamonds@Bi_2WO_6 nanocomposite from water and food samples.* Food Chem. 2024; 450:139351. http://doi.org/ 10.1016/j.foodchem.2024.139351

[11] Yağmuroğlu O. *Trace determination of nickel in Thymus serpyllum L. (wild thyme) tea with a matrix matching strategy by UV–Vis spectrometry after vortex-assisted DES/DPC-based microextraction*. Microchem J. 2025; 209:112755. http://doi.org/ 10.1016/j.microc.2025.112755

[12] Ozalp O, Issufo M, Soylak M. *Copper-chitosan modified with graphene oxide adsorbent for dispersive micro solid phase extraction of traces nickel from water and food samples*. J Food Compos Anal. 2026; 149:108676. http://doi.org/ 10.1016/j.jfca.2025.108676

[13] Fernandes BLM, Lisboa TP, de Oliveira WBV, Matos RC, Lowinsohn D. *A new sustainable approach using a composite material based on dimethylglyoxime and graphite immobilized on a 3D printed support for selective nickel detection*. J Electroanal Chem. 2023; 941:117538. http://doi.org/ 10.1016/j.jelechem.2023.117538

[14] Ghaemi M, Hajiaghababaei L, Tehrani RMA, Najafpour J, Shahvelayati AS. *Theoretical and experimental approaches to the use of benzoyl carbamothioyl alanine as a new ionophore for development of various mercury selective electrodes*. J Mol Liq. 2023; 370:121043. http://doi.org/ 10.1016/j.molliq.2022.121043

[15] Ghaemi M, Hajiaghababaei L, Najafpour J, Shahvelayati AS, Tehrani RMA. *Comparison of selectivity and sensitivity of various ferric selective electrodes prepared using N-((bis(dimethylamino)methylene) carbamothioyl) benzamide*. Phys Chem Chem Phys. 2024;26(27):18997-19007. http://doi.org/10.1039/D4CP01473A

[16] Sarvestani MRJ, Hajiaghababaei L, Najafpour J, Suzangarzadeh S. *1-(6-choloroquinoxaline-2-yl) hydrazine as an excellent ionophore for preparation of a cobalt selective electrode and potentiometric measuring of vitamin B12 in pharmaceutical samples*. Anal Bioanal Electrochem. 2018;10(6):675-698.

[17] Hajiaghababaei L, Sharafi A, Suzangarzadeh S, Faridbod F. *Mercury recognition: a potentiometric membrane sensor based on 4-(benzylideneamino)-3,4-dihydro-6-methyl-3-thioxo-1,2,4-triazin-5(2H) one*. Anal Bioanal Electrochem. 2013; 5:481-493.

[18] Svancara I, Vytras K, Kalcher K, Walcarius A, Wang J. *Carbon paste electrodes in modern electroanalysis*. Electroanalysis. 2009;21(1):7-28. http://doi.org/10.1002/elan.200804340

[19] Svancara I, Walcarius A, Kalcher K, Vytras K. *Carbon paste electrodes in facts, numbers and notes: a review on the occasion of the 50-years jubilee of carbon paste in electrochemistry and electroanalysis*. Electroanalysis. 2009;21(1):1-6. http://doi.org/10.1002/elan.200804341

[20] Kalcher K, Svancara I, Metelka R, Vytras K. *The carbon paste electrode: an evergreen electrode material in electroanalysis*. In: Electrochemistry. London: IntechOpen; 2019. http://doi.org/10.5772/intechopen.82102

[21] Tashkhourian J, Nami-Ana SF. *A new modified carbon paste electrode using N1-hydroxy-N1,N2-diphenylbenzamidine for the square wave anodic stripping voltammetric determination of Pb(II) in environmental samples.* Results Chem. 2022; 4:100049. http://doi.org/ 10.1016/j.rechem.2022.100049

[22] Beitollahi H, Tajik S, Nejad FG, Safaei M. *Recent advances in electrochemical sensing of anticancer drugs using carbon paste electrodes modified with nanomaterials: a review*. J Electrochem Sci Eng. 2023;13(4):789-812. http://doi.org/10.5599/jese.1234

[23] Anchidin-Norocel L, et al. *Development, optimization, characterization, and application of electrochemical biosensors for detecting nickel ions in food*. Biosensors. 2021;11(12):519.

[24] Mashhadizadeh MH, Sheikhshoaie I, Saeid-Nia S. *Nickel (II)-selective membrane potentiometric sensor using a recently synthesized Schiff base as neutral carrier*. Sens Actuators B Chem. 2003;94(3):241-246.

[25] Mohammed GI, Saber AL, El-Ghamry HA, Althakafy JT, Alessa H. *Ni (II)-selective PVC membrane sensor based on 1,2,4-triazole bis Schiff base ionophore: synthesis, characterization and application for potentiometric titration of Ni ions against EDTA*. Arab J Chem. 2021;14(7):103210.

[26] Sammes PG, et al. *Transition metal complexes of 1,10-phenanthroline: coordination and properties*. Chem Soc Rev. 1994.

[27] Ebadi S, Ghanbari K, Zahedi-Tabrizi M. *Development of an electrochemical sensor based on Ni-Bio-MOF and molecular imprinted polymer for diclofenac determination.* RSC Adv. 2025; 15:16983-16998.

[28] Singh, et al. *Nickel (II)-selective membrane electrode based on macrocyclic ligand*. Anal Chim Acta. 2001.

[29] Socaciu-Siebert A, Socaciu M, Socaciu C. *Computational insights and modeling of metabolic pathways of thymol and carvacrol chemical reactions: predictive modeling of medicinal plant biosynthesis*. J Agric Food Chem. 2023;71(15):6123-6135. http://doi.org/ 10.1021/acs.jafc.3c00123

[30] Kumar S, Singh R, Sharma A, et al. *Effect of molecular structure on the B3LYP-computed HOMO–LUMO gap: a structure–property relationship using atomic signatures*. ACS Omega. 2025;10(3):2799-2808. http://doi.org/10.1021/acsomega.4c08626

[31] Kumar S, et al. *Exploration of transition metal-hydride compounds: molecular structure, electronic properties, nonlinear optical characteristics, and reactivity of Cp-based binuclear ruthenium complexes.* J Organomet Chem. 2025; 1036:123707. http://doi.org/ 10.1016/j.jorganchem.2025.123707

[32] Deppmeier BJ, Driessen AJ, Hehre TS, Hehre WJ, Johnson JA, Klunzinger PE, et al. *Spartan'10, version 1.1.0. Irvine (CA)*: Wavefunction Inc.; 2011.

[33] *Current trends in computational quantum chemistry studies on antioxidant radical scavenging activity*. J Chem Inf Model. 2022;62(9):2055-2082. http://doi.org/ 10.1021/acs.jcim.2c00104

[34] Dennington RD II, Keith TA, Millam JM. GaussView, version 5. Shawnee Mission (KS): Semichem Inc.; 2009.

[35] Becke AD. *Density-functional thermochemistry. III. The role of exact exchange*. J Chem Phys. 1993;98(7):5648-5652. http://doi.org/10.1063/1.464913

[36] Becke AD. *Density-functional exchange-energy approximation with correct asymptotic behavior*. Phys Rev A. 1988;38(6):3098-3100. http://doi.org/10.1103/PhysRevA.38.3098

[37] Lee C, Yang W, Parr RG. *Development of the Colle-Salvetti correlation-energy formula into a functional of the electron density*. Phys Rev B. 1988;37(2):785-789. http://doi.org/10.1103/PhysRevB.37.785

[38] Frisch MJ, Trucks GW, Schlegel HB, Scuseria GE, Robb MA, Cheeseman JR, et al. Gaussian 09, Revision A.1. Wallingford (CT): Gaussian Inc.; 2009.

[39] El Ayadi M, El Mouchtari EM, Robert-Peillard F, Bonne D, Humbel S, Boudenne JL, et al. *DFT study of the structural, electronic, and nonlinear optical properties of perfluorinated circumanthracene derivatives.* Heliyon. 2025;11(2): e42185. http://doi.org/ 10.1016/j.heliyon. 2025.e42185

[40] Tomasi J, Mennucci B, Cammi R. *Quantum mechanical continuum solvation models*. Chem Rev. 2005;105(8):2999-3094

[41] Al-Ghamdi AA, Al-Ghamdi MA, Al-Ghamdi SA, et al. *DFT exploration of metal ion–ligand binding: toward rational design of chelating agent in semiconductor manufacturing*. Molecules. 2024;29(2):308. http://doi.org/10.3390/molecules29020308

[42] Sengupta P, et al. *Development of reusable screen-printed ion-selective electrodes with calibration-free operation. Sens Bio-Sens Res*. 2025; 49:100367. http://doi.org/ 10.1016/j.sbsr.2025.100367

[43] Gao Y, et al. *Benchmarking first-principles reaction equilibrium composition prediction. Molecules*. 2023;28(9):3649. http://doi.org/10.3390/molecules28093649

[44] Barroso J. Useful thermochemistry from Gaussian calculations. Dr Joaquin Barroso's Blog; 2024-2025.

[45] Morawska K, et al. *Application of ionic liquids in ion-selective electrodes and reference electrodes: a review*. ChemPhysChem. 2024;25(5): e202300818. http://doi.org/10.1002/cphc.202300818

[46] Al-Ghamdi AA, et al. *Electrochemical investigation of oxytrol in fizzy drinks and juices via graphene and polymer printed PVC by ANOVA and design expert*. Sci Rep. 2025; 15:12803. http://doi.org/10.1038/s41598-025-12803-z

[47] Wang Y, et al. *Recent developments and challenges in solid-contact ion-selective electrodes*. Sensors. 2024;24(13):4289. http://doi.org/10.3390/s24134289

[48] Krajewski M, et al. *Preparation of a new active component 1,10-$B_{10}H_8(S(C_{18}H_{37})_2)_2$ for potentiometric membranes for the determination of terbinafine hydrochloride.* Inorganics. 2025;13(2):35. http://doi.org/10.3390/inorganics13020035

[49] Khan A, et al. *An empirical model of ion-selective organic electrochemical transistors for potentiometric sensing*. In: 2024 IEEE SENSORS. Kobe (Japan): IEEE; 2024. p. 1-4.

[50] Ganjali MR, et al. *An electrochemical Ni(II)-selective sensor based on a newly synthesized dioxime derivative as a neutral ionophore*. Sens Actuators B Chem. 2006;113(1):40-46. http://doi.org/ 10.1016/j.snb.2005.02.026

[51] Gupta VK, et al. *Nickel analysis in real samples by Ni2+ selective PVC membrane electrode based on a new Schiff base*. Mater Sci Eng C. 2013;33(8):4882-4888. http://doi.org/ 10.1016/j.msec.2013.08.010

[52] Rezaei B, Meghdadi S, Zarif Afrah V. *Nickel (II) selective PVC-based membrane sensor using a Schiff base*. Int J Spectrosc. 2011; 2011:746372. http://doi.org/10.1155/2011/746372

[53] Kumar KG, John KS. *Ni (II)-selective PVC membrane sensor based on 1,2,4-triazole bis Schiff base ionophore: synthesis, characterization and application for potentiometric titration of Ni2+ ions against EDTA*. Arab J Chem. 2022;15(6):103761. http://doi.org/ 10.1016/j.arabjc.2022.103761